P6A.4

Fine structure of vertical motion in the stratiform precipitation region observed by Equatorial Atmosphere Radar (EAR) in Sumatra, Indonesia

Noriyuki, NISHI*, Graduate School of Science, Kyoto University, JAPAN
Masayuki, YAMAMOTO, Research Institute for Sustainable Humanosphere, Kyoto University, JAPAN
Toyoshi SHIMOMAI, Interdisciplinary Faculty of Science and Engineering, Shimane University, JAPAN
Atsushi, HAMADA, Graduate School of Science, Kyoto University, JAPAN
Shoichiro, FUKAO, Research Institute for Sustainable Humanosphere, Kyoto University. JAPAN

1. Introduction

The Equatorial Atmosphere Radar (EAR) is a VHF Doppler radar installed at the Equatorial Atmosphere Observatory, Kototabang (0.2˚S, 100.32˚E, 865 m MSL) (Fukao et al. 2003), which has enabled the observation of vertical motion (W) with fine time (3 minutes) and vertical (150 m) resolutions. The present paper describes the fine structure of W within the stratiform precipitation region of tropical mesoscale cloud clusters.

In a mesoscale cloud cluster, the stratiform precipitation region mainly consisting of nimbostratus occupies most of the area. Vertical motions are closely related to dynamics and physics within nimbostratus (Houze 1993). On the other hand, the magnitude of upward motion affects the size and lifetime of nimbostratus, because it sustains precipitation particles within the clouds. Houze (1989) collected the results of past observational studies and demonstrated that upward motion in the stratiform precipitation region of tropical mesoscale cloud clusters was about 10-20 cm s^{-1}. However, the vertical profile of W shown in most of the previous studies was computed only by indirect methods, such as the vertical integration of horizontal divergence observed by radiosonde or weather radar.

Indirect methods for the computation of W have been shown to have difficulties in describing fine structure of W in tropical nimbostratus, as mentioned below. Estimation of W from radiosonde data is limited to a large-area average. Weather radar cannot estimate W without precipitation particles even inside clouds and needs to hypothesize the boundary condition when integrating horizontal divergence vertically.

On the other hand, VHF Doppler radar can directly observe W above the radar. VHF Doppler radar receives an echo from atmospheric turbulence with a scale of several meters (half of its wavelength), in both clear and cloudy regions (Fukao et al. 1985). There have been several studies on the distribution of W in the stratiform precipitation region using VHF Doppler radars installed in the Pacific region (Balsley et al. 1988, Cifelli and Rutledge 1994, Kumar et al. 2001). They showed statistics of the vertical distribution of W and several examples of the distribution of W in regions such as western and central Pacific, northern Australia, and India.

It is of interest to detail more precise time-height structure inside the clouds within the stratiform precipitation region with finer vertical and time resolutions than previous studies.

*****_Corresponding author address:_ NISHI Noriyuki, Division of Earth and Planetary Science, Graduate School of Science, Kyoto University, Kitashirakawa Oiwake, Sakyo, Kyoto 606-8502 JAPAN. E-mail: nishi@kugi.kyoto-u.ac.jp

2. Data description

During November 2003, the EAR was operated with an additional vertical observation mode to intensively monitor W (hereafter referred to as the vertical wind mode). Estimated error in W is 2.6 cm s^{-1} even in considerably turbulent conditions for a Doppler width of 0.5 m s^{-1} in the stratiform precipitation region.

Geostationary Operational Environmental Satellite 9 (GOES-9) black body temperature (Tbb) data in the infrared (IR1: 10.2-11.2 μm) range, with a horizontal 0.05˚ and one hour resolutions are utilized. The Tbb data and NCEP/DOE Reanalysis 2 were used to estimate the cloud top heights, which is referred to as the “Tbb cloud top index”.

A weather radar operated at 9.74-GHz frequency installed at Kototabang was used to observe the vertical distribution of precipitation particles and to identify the stratiform rain region by detecting the bright band near the melting level. Due to the maximum elevation angle of 29.5˚, the vertical profile of the weather radar reflectivity factor (hereafter referred to as Z) was calculated by using the 29.5˚-elevation beam. The ratio of Z over noise level in a scanned circle was also calculated and shown in the figures.

3. Results

The cloud clusters that accompany active nimbostratus were objectively selected (6, 8 and 20 November). Basically, if a bright band is detected around the level of 0˚C, the region is recognized as a stratiform precipitation region (Rosenfeld et al. 1995). In this study, clouds embedded in the middle and upper troposphere of a stratiform precipitation region is classified as the

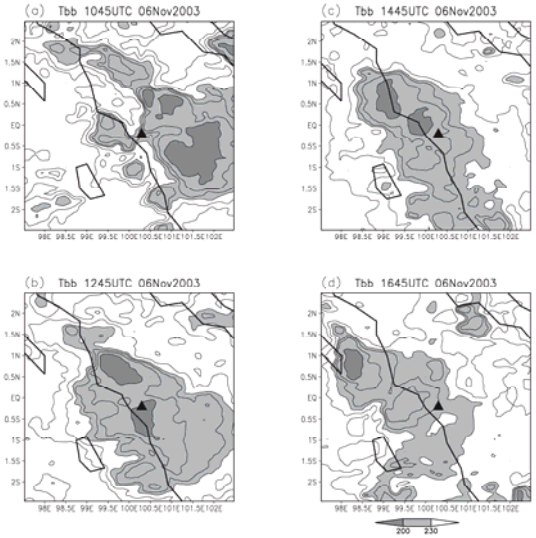

Fig. 1 Longitude-latitude sections of Tbb observations by GOES-9 (averaged in 0.15˚ box) displaying the passage of a mesoscale cloud cluster over Kototabang at (a) 1045 UTC, (b) 1245 UTC, (c) 1445 UTC, and (d) 1645 UTC on 6 November 2003. The triangle at the center of the map indicates the location of Kototabang. Light shade denotes the regions of TBB less than 230K, while the dark shade indicates the regions of TBB less than 200K. The contour levels are 190, 200, 210, 220, 230, 250, 270, and 290 K. The thick contour lines denote the coastlines.

nimbostratus.

Figure 1 shows the time sequence of a mesoscale cloud cluster passing over Kototabang in the evening of 6 November. The Tbb at Kototabang reaches a minimum value of less than 200 K around 1245 UTC. The region of the lowest Tbb values moves to the northwest of Kototabang by 1645 UTC, while the relatively low Tbb values of about 230 K still surround the Kototabang region.

Figure 2 shows the time series of W, the Tbb cloud top index, Z and surface rain at Kototabang. Until a bright band appears at around 5 km at 1340 UTC (Fig. 2b), convective activity appears to pass over the Kototabang region, since the Tbb cloud top index reaches 15 km (1245 UTC), and W has a magnitude greater than 1 m s^{-1} (e.g., 8 km at 1100Z and 4 km at 1310Z).

After the passage of the possible convective activity, a bright band appears after 1340 UTC, and continues until 1900 UTC although gradually becoming weak in the later stage. This period (1340-1900 UTC) is regarded as a stratiform precipitation region. The Tbb cloud top index is near 14 km at 1345 UTC, and gradually decreases

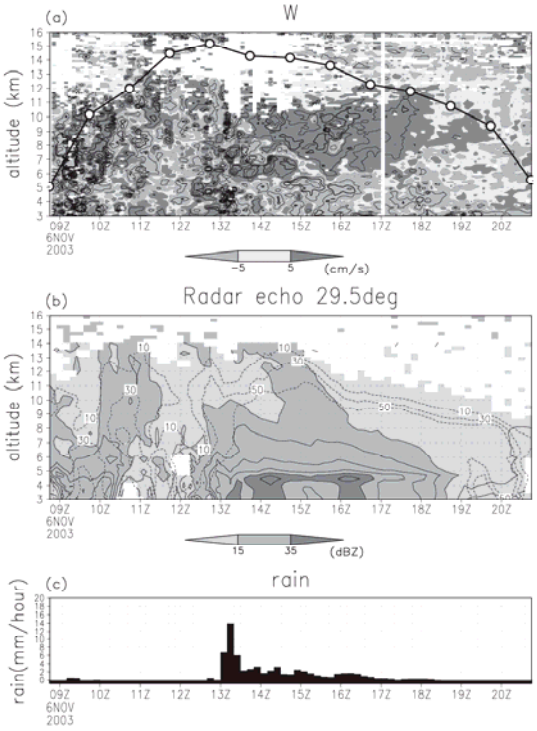

Fig. 2 Vertical motion and cloud variables when a cloud cluster passes over Kototabang on 6 November 2003. (a) Shading and contours show 12-minute averaged vertical motion (cm s^{-1}) observed by the EAR. White area indicates missing data. Thick contour levels are -300 -200, -100, -40, 40, 100, 200 and 300 cm s^{-1}; thin contour levels are from -80 cm s^{-1} to +80 cm s^{-1} with a 20 cm s^{-1} interval except the level of 0 cm s^{-1}. The values of Tbb cloud top index inferred from GOES-9 Tbb data are shown by the open circles and bold line (see Section 2 for detail). Altitude of 0 km is MSL. (b) Radar reflectivity factor (Z) derived from the weather radar around Kototabang. Shading and solid contour lines show the averaged Z around EAR (dBZ). The contour interval is 5 dBZ. The broken lines indicate the rate (%) of returned reflectivity in a scanned circle (see Section 2 for detail). (c) Ten minute accumulated rain amounts by an optical rain gauge (mm $hour^{-1}$)

to 12 km at 1645 UTC. The spatial distribution of Tbb is rather uniform around Kototabang (Fig. 1). Surface rain is observed during almost all of the stratiform precipitation period, until 1820 UTC, and the rate of rainfall is less than 4 mm $hour^{-1}$. This weak rate of surface rain supports the fact that this period falls under stratiform precipitation conditions (Balsley et al. 1988).

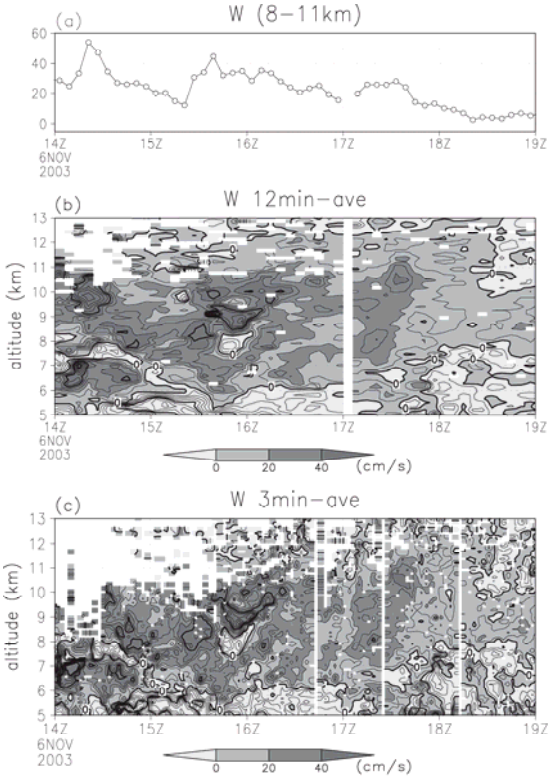

Fig. 3 Fine structure of the vertical motion (cm s^{-1}) when a cloud cluster passes over Kototabang on 6 November 2003. (a) Vertical motion (shown in (b)) averaged in 8-11-km height range. (b) Twelve minute average of vertical motion. White areas indicate missing data. Thin contours are for each 10 cm s^{-1} between -100 and 100 cm s^{-1}, and thick contours are for each 50 cm s^{-1} between -300 and 300 cm s^{-1}. (c) Three minute average of vertical motion. Contours and shading patterns are same as (b).

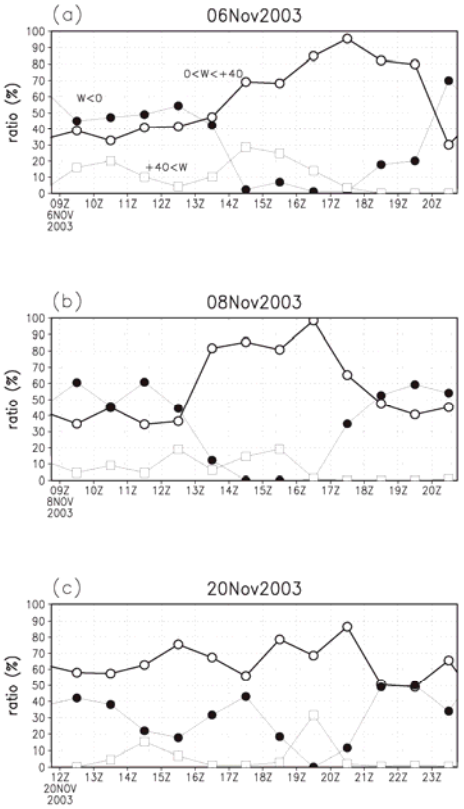

Fig. 4 The frequency (see text for detail) of weak upward motion (smaller than 40 cm s^{-1}, thick line with open circle), strong upward motion (larger than 40 cm s^{-1}, thin line with open square) and downward motion (thin line with closed circle) for (a) the 6 November cloud cluster, (b) the 8 November cloud cluster, and (c) the 20 November cloud cluster in 8-11 km.

A noticeable feature in the nimbostratus is the continuous gentle upward motion with small fluctuations in the later stage of the stratiform precipitation region. In examining the stratiform precipitation region in detail, a slight increase in Z and the surface rain can be detected around 1600 UTC, as well as a rather strong upward motion of about 1 m s^{-1} and downward motions in the 6-12 km height range. At this time, convective clouds could possibly be embedded in the stratiform precipitation region. After this event (around 1600 UTC), gentle upward motions with small fluctuations are continuously observed in the middle and upper troposphere.

Around 1630 UTC, the layer of gentle upward motion, where the value of W is positive and smaller than 40 cm s^{-1} over most of the range, has a large vertical extent (6.0-11.0 km height range). Fig. 3b is presented to show the temporal distribution of the fine structure of W in the nimbostratus. The vertical range of the layer seems to be lifted to 8.0-12.5 km around 1830 UTC. During 1630-1830 UTC, upward motions of greater than 40 cm s^{-1} and downward motions are almost absent in the height range. After 1830 UTC, the range of weak upward motion is dissolving.

The most striking feature among the various structures of W in the nimbostratus is well shown around 8 – 11 km during 1630 – 1830 UTC. Only a few contours are drawn at the 10 cm s^{-1} interval in Fig. 3b; both the time and height variations of W are inactive over this period. Figure 3a exhibits the vertically averaged W in the nimbostratus (8-11 km). The vertically averaged W is rather constant in most of the stratifrom precipitation period; it is in 15-40 cm s^{-1} range between 1430-1800 UTC except large fluctuation around 1530 UTC. However, the variability inside nimbostratus shown in Fig. 3b is reduced around 1630 UTC. The gentle upward motion is strongly contrasted versus the early stage of the stratiform precipitation region (1400-1600 UTC). Another dataset with a finer time resolution of 3-minute was inspected (Fig. 3c), though the data are missing for some regions.

Significant fluctuations of W in the dataset with a time scales of less than 12 minutes were not detected.

Figure 4a shows the hourly histogram of W in height range of 8-11 km on 6 November with 12-minute and 150-m height resolutions. The number of values of W was counted during one hour. Prior to 14 UTC, the frequency of downward motion is almost the same as that of upward motion, which suggests a rather convective feature. After 14 UTC, the frequency of stronger upward motion of greater than 40 cm s^{-1} slightly increases, whereas that of downward motion becomes less than 20 %. During the later stage of the stratiform precipitation region (17 to 18 UTC), the frequency of weak upward motion (0-40 cm s^{-1}) exceeds 95 %. Most of the weak upward motions during the 17-18 UTC period are of a gentle nature in nimbostratus. Similar gentle upward motions are detected in the clusters on 8 and 20 November (Figure 4). The details of these cases are described in Nishi et al. (2007).

The time resolution of 3 minutes is sufficiently smaller than the scale of buoyancy period (7-10 minutes): the lower limit of internal gravity wave. If 10-15 m s^{-1} is adopted as a typical moving speed of a cloud system, the horizontal resolutions would be 1.8-2.7 km, in 3-minute data. It is probably smaller than scale of each cumulonimbus cell.

4. Discussion

To keep a gentle upward motion with small fluctuation for a long period, needed are both conditions: (1) the dominance of processes to maintain slow upward motion in a wide region and (2) the suppression of processes that make short-period and/or strong vertical motion.

Latent heat release resulting from deposition growth is one of the most plausible causes for the uniform upward motion. If the air around ice particles is supersaturated to the ice, much vapor can be deposited on the ice particles. Latent heat release by deposition can occur over large part of the height range and enables to develop a widely extended mesoscale low-pressure region in the nimbostratus (e.g. Houze 1989).

Gravity wave with time and spatial scale comparable or larger than the extension of nimbostratus region is another candidate. They are induced by continuous heating produced by the total effects of the cumulonimbi that occur repeatedly and frequently in the convective region. When the horizontal and vertical scales of gravity waves are large enough, one large nimbostratus region can be in one upward phase region of the wave.

On the other hand, the following processes tend to make fluctuations with short time scale. One process is old cells, which have their origin in the convective region and are often observed even far region from convective part in a strong vertical shear condition (e.g. Houze 1993), in the upper part of nimbostratus. If these cells have enough buoyancy, they make a strong upward motion with small scale. Another one is the seeder-feeder mechanism that sometimes produces a rainband structure. Latent heat is released by the freezing of supercooled raindrops when falling ice particles come in contact with the drops (e.g., Hobbs et al. 1980). This may happen rather in the lower part of nimbostratus, and induce thermal instability resulting in a small-scale cell-like structure. Gravity waves with the smaller time scale than duration of the nimbostratus, which are produced possibly by each convective cloud and propagate to the stratiform part, also create large variability. These processes should be suppressed when gentle upward motions without small-scale fluctuation dominate in the stratiform precipitation regions.

In the present study, it is not sure which processes are active and/or suppressed in the nimbostratus due to the lack of information on the cloud microphysics and horizontal distribution of the cloud systems.

5. Summary

The fine structures of vertical motion (W) in three mesoscale cloud clusters were investigated by EAR. By applying an observational mode to intensively observe in the vertical direction, W was observed with sufficient accuracy (better than 5 cm s^{-1}), and fine resolutions (3 minutes and 12 minutes; 150 m in the vertical direction) to examine weak vertical motions in nimbostrarus.

The passage of several typical isolated mesoscale cloud clusters was observed. In the later two or three hours of the stratiform precipitation period, the gentle upward motion with small time and height fluctuations was observed in three cases (6, 8, and 20 November). Over approximately three to five kilometers from the middle to upper troposphere, W had weak positive values (0-40 cm s^{-1}) almost continuously with hardly any upward motions greater than 40 cm s^{-1}, and any downward motion. Within these regions, the time and height fluctuations of W were small. The uniqueness of this study is quantitative description on the gentle upward motion with small fluctuation. The important point is not only that *averaged* value of W was observed to be on the order of 10 cm s^{-1} as is well known, but also that the uniform weak upward motion was found to continue in rather deep height range over two to three hours in the stratiform precipitation region.

REFERENCES

Balsley, B. B., W. L., Ecklund, D. A., Carter, A. C., Riddle, and K. S., Gage, 1988: Average vertical motions in the tropical atmosphere observed by a radar wind profiler on Pohnpei (7°N Latitude, 157°E Longitude). J. Atmos. Sci., **45**, 396-405.

Cifelli, R., S. A., Rutledge, 1994: Vertical motion

structure in Maritime Continent mesoscale convective systems: Results from a 50-MHz profiler. J. Atmos. Sci., **51**, 2631-2652.

Fukao, S., H. Hashiguchi, M. Yamamoto, T. Tsuda, T. Nakamura, M. K. Yamamoto, T. Sato, M. Hagio, and Y. Yabugaki, 2003: Equatorial Atmospheric Radar (EAR): System description and first results. Radio. Sci., **38**(3), 1053, doi:10.1029/2002RS002767, 2003.

Fukao, S., K. Wakasugi, T. Sato, S. Morimoto, T. Tsuda, I. Hirota, I. Kimura, and S. Kato, 1985: Direct measurement of air and precipitation particle motion by very high frequency Doppler radar. Nature, **316**, 712-714.

Hobbs, P. V., T. J. Matejka, P. H. Herzegh, J. D. Locatelli, and R. A. Houze, Jr., 1980: The mesoscale and microscale structure and organization of clouds and precipitation in midlatitude cyclones. I: A case study of a cold front. J. Atmos. Sci., **37**, 568-596.

Houze, R. A., Jr., 1989: Observed structure of mesoscale convective systems and implications for large-scale heating. Quart. J. of Roy. Meteor. Soc., **115**, 425-461.

Houze, R. A., Jr., 1993: *Cloud dynamics.* 573pp., Academic, San Diego, Calif.

Kumar, Y. Bhavani, Kumar, V. Siva, Jain, A. R. and Rao, P. B., 2001: MST radar and polarization lindar observations of tropical cirrus. Ann. Geophys., **19,** 873-882.

Nishi, N., M. K. Yamamoto, T. Shimomai, A. Hamada, and S. Fukao, 2007: Fine structure of vertical motion in the stratiform precipitation region observed by a VHF Doppler radar installed in Sumatra, Indonesia. J. Applied Meteor. Climatology, **46**, 522--537.

Rosenfeld, D., E. Amitai, D. B. Wolff, 1995: Classification of rain regimes by the three-dimensional properties of reflectivity fields. J. Appl. Meteorol., **34,** 198-211.